

mice with or without the C57Bl/Ka-Ly5.2 recipient bone marrow cells¹. Reconstitution of donor (Ly5.1) myeloid and lymphoid cells was monitored by staining blood cells with antibodies against Ly5.1, CD3, B220, Mac-1 and Gr-1. The secondary bone marrow transplant was performed with 10⁷ whole bone marrow cells from mice reconstituted with *Bmi-1*^{+/+} or *Bmi-1*^{-/-} fetal liver cells.

Retroviral gene transfer of HSCs

Mouse stem cell viruses expressing mouse *p16*^{Ink4a} or *p19*^{Af} cDNAs together with GFP were produced using Phoenix ecotropic packaging cells²⁸. Infection of HSCs was done as described²⁹ except that three cycles of infections were performed. After 48 h, single GFP-positive cells were sorted into a 96-well plate containing 100 µl HSC medium²⁹ and grown for 7 days. Each well was scored for the presence of GFP-positive cells by observation with a fluorescence microscope.

Received 10 February; accepted 19 March 2003; doi:10.1038/nature01587.
Published online 20 April 2003.

1. Morrison, S. J. & Weissman, I. L. The long-term repopulating subset of hematopoietic stem cells is deterministic and isolatable by phenotype. *Immunity* **1**, 661–673 (1994).
2. van der Lugt, N. M. *et al.* Posterior transformation, neurological abnormalities, and severe hematopoietic defects in mice with a targeted deletion of the *bmi-1* proto-oncogene. *Genes Dev.* **8**, 757–769 (1994).
3. Ramalho-Santos, M. *et al.* 'Stemness': transcriptional profiling of embryonic and adult stem cells. *Science* **298**, 597–600 (2002).
4. Park, I.-K. *et al.* Molecular cloning and characterization of a novel regulator of G-protein signaling from mouse hematopoietic stem cells. *J. Biol. Chem.* **276**, 915–923 (2001).
5. Park, I. K. *et al.* Differential gene expression profiling of adult murine hematopoietic stem cells. *Blood* **99**, 488–498 (2002).
6. Lessard, J., Baban, S. & Sauvageau, G. Stage-specific expression of Polycomb group genes in human bone marrow cells. *Blood* **91**, 1216–1224 (1999).
7. Kiyono, T. *et al.* Both Rb/p16^{INK4a} inactivation and telomerase activity are required to immortalize human epithelial cells. *Nature* **396**, 84–88 (1998).
8. van der Lugt, N. M. T., Alkema, M., Berns, A. & Deschamps, J. The Polycomb-group homolog *Bmi-1* is a regulator of murine Hox gene expression. *Mech. Dev.* **58**, 153–164 (1996).
9. Akashi, K. *et al.* Transcriptional accessibility for genes of multiple tissues and hematopoietic lineages is hierarchically controlled during early hematopoiesis. *Blood* **101**, 383–389 (2003).
10. Morrison, S., Hemmati, H., Wandycz, A. & Weissman, I. The purification and characterization of fetal liver hematopoietic stem cells. *Proc. Natl Acad. Sci. USA* **92**, 10302–10306 (1995).
11. Wright, D. E. *et al.* Hematopoietic stem cells are uniquely selective in their migratory response to chemokines. *J. Exp. Med.* **195**, 1145–1154 (2002).
12. Mahmoudi, T. & Verrijzer, C. P. Chromatin silencing and activation by Polycomb and trithorax group proteins. *Oncogene* **20**, 3055–3066 (2001).
13. Weber, J. D. *et al.* Nucleolar Arf sequesters Mdm2 and activates p53. *Nature Cell Biol.* **1**, 20–26 (1999).
14. Jacob, J. *et al.* The oncogene and Polycomb-group gene *bmi-1* regulates cell proliferation and senescence through the *ink4a* locus. *Nature* **397**, 164–168 (1999).
15. Quelle, D. E., Zindy, F., Ashmun, R. A. & Sherr, C. J. Alternative reading frames of the INK4a tumour suppressor gene encode two unrelated proteins capable of inducing cell cycle arrest. *Cell* **84**, 993–1000 (1995).
16. Antonchuk, J., Sauvageau, G. & Humphries, R. K. HOXB4 overexpression mediates very rapid stem cell regeneration and competitive hematopoietic repopulation. *Exp. Hematol.* **29**, 1125–1134 (2002).
17. Lawrence, H. J. *et al.* Mice bearing a targeted interruption of the homeobox gene HOXA9 have defects in myeloid, erythroid, and lymphoid hematopoiesis. *Blood* **89**, 1922–1930 (1997).
18. Christensen, J. L. & Weissman, I. L. Flk-2 is a marker in hematopoietic stem cell differentiation: a simple method to isolate long-term stem cells. *Proc. Natl Acad. Sci. USA* **98**, 14541–14546 (2001).
19. Zhang, Y., Xiong, Y. & Yarbrough, W. G. ARF promotes MDM2 degradation and stabilizes p53: ARF-INK4a locus deletion impairs both the Rb and p53 tumour suppression pathways. *Cell* **92**, 725–734 (1998).
20. Shivdasani, R., Mayer, E. & Orkin, S. Absence of blood formation in mice lacking the T-cell leukaemia oncogene tal-1/SCL. *Nature* **373**, 432–434 (1995).
21. Porcher, C. *et al.* The T cell leukemia oncogene SCL/tal-1 is essential for development of all hematopoietic lineages. *Cell* **86**, 47–57 (1996).
22. Antonchuk, J., Sauvageau, G. & Humphries, R. K. HOXB4-induced expansion of adult hematopoietic stem cells *ex vivo*. *Cell* **109**, 39–45 (2002).
23. Domen, J., Cheshier, S. H. & Weissman, I. L. The role of apoptosis in the regulation of hematopoietic stem cells: overexpression of BCL-2 increases both their number and repopulation potential. *J. Exp. Med.* **191**, 253–264 (2000).
24. Nichogiannopoulou, A. *et al.* Defects in hemopoietic stem cell activity in Ikaros mutant mice. *J. Exp. Med.* **190**, 1201–1214 (1999).
25. Fisher, R. C., Lovelock, J. D. & Scott, E. W. A critical role for PU.1 in homing and long-term engraftment by hematopoietic stem cells in the bone marrow. *Blood* **94**, 1283–1290 (1999).
26. Cheng, T. *et al.* Hematopoietic stem cell quiescence maintained by p21^{cip1/waf1}. *Science* **287**, 1804–1808 (2000).
27. Ohta, H. *et al.* Polycomb group gene *rae28* is required for sustaining activity of hematopoietic stem cells. *J. Exp. Med.* **195**, 759–770 (2002).
28. Pear, W., Nolan, G., Scott, M. & Baltimore, D. Production of high-titer helper-free retroviruses by transient transfection. *Proc. Natl Acad. Sci. U.S.A.* **90**, 8392–8396 (1993).
29. Cotta, C., Swindle, C., Weissman, I. L. & Klug, C. A. *Retroviral Transduction of FACS-Purified Hematopoietic Stem Cells* (eds Klug, C. A. & Jordan, C. T.) 243–252 (Humana Press, Totowa, New Jersey, 2001).
30. Lessard, J. & Sauvageau, G. *Bmi-1* determines the proliferative capacity of normal and leukaemic stem cells. *Nature* advance online publication, 20 April 2003 (doi: 10.1038/nature01572).

Supplementary Information accompanies the paper on www.nature.com/nature.

Acknowledgements We thank T. Magnuson and C. Klug for providing *Bmi-1*^{+/-} mice and the MSCV plasmid, respectively; and the Flow Cytometry Core and the Microarray Core at the University of Michigan for their work. The Microarray Core is supported in part by a University of Michigan's Cancer Center Support Grant from the NIH. This work is supported by grants from the NIH.

Competing interests statement The authors declare that they have no competing financial interests.

Correspondence and requests for materials should be addressed to M.F.C. (mclarke@umich.edu).

DNA helicase Srs2 disrupts the Rad51 presynaptic filament

Lumir Krejci^{*†}, Stephen Van Komen^{*†}, Ying Li[‡], Jana Villemain^{*}, Mothe Sreedhar Reddy^{*}, Hannah Klein[§], Thomas Ellenberger[‡] & Patrick Sung^{*}

* Institute of Biotechnology and Department of Molecular Medicine, University of Texas Health Science Center at San Antonio, 15355 Lambda Drive, San Antonio, Texas 78245, USA

‡ Department of Biological Chemistry and Molecular Pharmacology, Harvard Medical School, Boston, Massachusetts 02115, USA

§ Department of Biochemistry, New York University School of Medicine, New York, New York 10016, USA

† These authors contributed equally to the work

Mutations in the *Saccharomyces cerevisiae* gene *SRS2* result in the yeast's sensitivity to genotoxic agents, failure to recover or adapt from DNA damage checkpoint-mediated cell cycle arrest, slow growth, chromosome loss, and hyper-recombination^{1,2}. Furthermore, double mutant strains, with mutations in DNA helicase genes *SRS2* and *SGS1*, show low viability that can be overcome by inactivating recombination, implying that untimely recombination is the cause of growth impairment^{1,3,4}. Here we clarify the role of *SRS2* in recombination modulation by purifying its encoded product and examining its interactions with the Rad51 recombinase. *Srs2* has a robust ATPase activity that is dependent on single-stranded DNA (ssDNA) and binds Rad51, but the addition of a catalytic quantity of *Srs2* to Rad51-mediated recombination reactions causes severe inhibition of these reactions. We show that *Srs2* acts by dislodging Rad51 from ssDNA. Thus, the attenuation of recombination efficiency by *Srs2* stems primarily from its ability to dismantle the Rad51 presynaptic filament efficiently. Our findings have implications for the basis of Bloom's and Werner's syndromes, which are caused by mutations in DNA helicases and are characterized by increased frequencies of recombination and a predisposition to cancers and accelerated ageing⁵.

We have been unable to overexpress *Srs2* protein significantly in yeast, suggesting that this protein is unstable in, and/or toxic to, yeast cells. We therefore turned to *Escherichia coli* and an inducible T7 promoter as vehicle for *Srs2* expression. *Srs2* could be revealed by Coomassie Blue staining of *E. coli* extracts and by immunoblotting with antibodies against *Srs2* (Fig. 1a). We subjected *E. coli* lysate to precipitation with ammonium sulphate and a five-step chromatographic fractionation scheme to purify *Srs2* to near-homogeneity (Fig. 1b). Purified *Srs2* has a robust ssDNA-dependent ATPase activity ($k_{cat} \geq 2,500 \text{ min}^{-1}$) and a DNA helicase activity⁶ that is fuelled by ATP hydrolysis (Fig. 1c).

Previous studies have unveiled an anti-recombination function in *SRS2* and a genetic interaction with *RAD51* (refs 7–9). We investigated whether *Srs2* protein interacts physically with Rad51 protein, and also tested its effect on the Rad51 recombinase activity¹⁰. To

examine whether Srs2 associates with Rad51, we coupled the latter to Affi-gel 15 beads and used the resulting matrix to bind Srs2. As shown in Fig. 1d, Srs2 was retained on the Affi-Rad51 beads, but no binding of Srs2 to bovine serum albumin (BSA) immobilized on Affi-beads (Affi-BSA) was detected. An interaction between Rad51 and two carboxy-terminal fragments of Srs2 was seen in the two-hybrid assay in yeast (Fig. 1e). We were unable to detect significant interaction between Rad51 and full-length Srs2 in this assay, which could be the result of low expression of full-length Srs2.

We next tested the effect of Srs2 on the Rad51-mediated homologous pairing and strand exchange reaction that serves to join recombining DNA molecules^{10,11}. For this, we employed a commonly used assay in which Rad51 and the heterotrimeric ssDNA-binding factor RPA are incubated with ssDNA and ATP to form a Rad51-ssDNA nucleoprotein filament¹¹⁻¹³. Such a filament, often called the presynaptic filament¹¹⁻¹³, is then incubated with the homologous linear duplex (Fig. 2Aa). Pairing between the DNA substrates yields a joint molecule, which is further processed by DNA strand exchange to nicked circular duplex (Fig. 2Aa, b). As shown in Fig. 2Ac, d, the addition of a catalytic quantity of Srs2 strongly suppressed the homologous pairing and strand exchange reaction.

To characterize its anti-recombination activity further, Srs2 was added to D-loop reactions in which pairing of a ³²P-labelled 90-mer oligonucleotide with a homologous duplex target is mediated by the combination of Rad51 and Rad54 proteins^{14,15} (Fig. 2Ba). As reported previously¹⁴⁻¹⁶, efficient D-loop formation was catalysed by Rad51 and Rad54 (Fig. 2Bb, d). As expected, the inclusion of Srs2 decreased the level of D-loop formation (Fig. 2Bb, d). RPA enhanced D-loop formation in the absence of Srs2 (Fig. 2Bc, d), but the inhibitory effect of Srs2 became much more pronounced when RPA was present. We provide an explanation below for this observation.

We considered the possibility that suppression of recombination by Srs2 might result from the dissociation of DNA joints by its helicase activity. To address this, D-loop was formed with Rad51/Rad54 and then Srs2 was added. Srs2 was incapable of dissociating the preformed D-loop, regardless of the presence or absence of RPA

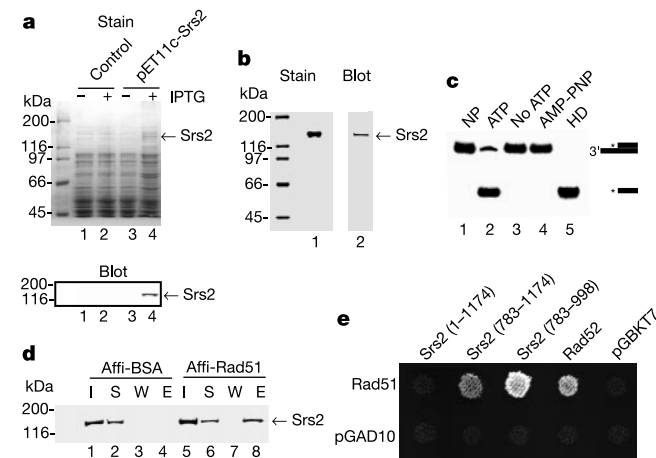


Figure 1 Purification and characterization of Srs2. **a**, Extracts from *E. coli* cells harbouring pET11c::Srs2 and the control vector pET11c grown with or without isopropyl β-D-thiogalactoside (IPTG) were analysed by SDS-PAGE and immunoblotting. **b**, Purified Srs2 was analysed by SDS-PAGE (2 μg) and immunoblotting (20 ng). **c**, DNA unwinding by Srs2 occurs with ATP but not without it or with AMP-PNP. The substrate was also incubated alone (NP) or boiled (HD) for 1 min. **d**, Srs2 was mixed with Affi-Rad51 and Affi-BSA beads. The input (I), supernatant (S), wash (W) and SDS eluate (E) were immunoblotted. **e**, Full-length and truncated versions of Srs2 were tested for two-hybrid interaction with Rad51. Empty vectors and Rad52 were included as controls.

(Fig. 3A), suggesting that suppression of the recombination reaction does not stem from the unwinding of DNA by Srs2.

Several approaches were used to test the idea that Srs2 inhibits Rad51 recombinase function by disrupting the presynaptic filament. In doing so, we reasoned that disruption of the presynaptic filament would yield free Rad51 molecules that could be trapped on duplex DNA (dsDNA). The binding of Rad51 to topologically relaxed dsDNA induces lengthening of the DNA^{17,18} that can be monitored as a change in the DNA linking number on treatment with topoisomerase I (Fig. 3Ba). The product of this reaction is an underwound species referred to as form U (Fig. 3Bb, lane 4). RPA and Srs2 do not catalyse the formation of form U (Fig. 3Bb, lane 8), and these proteins have no effect on the formation of form U by Rad51 (Fig. 3Bb, compare lanes 6 and 4). The presynaptic filament consisting of Rad51-ssDNA does not make form U (Fig. 3Bc, lane 3). The addition of Srs2 to the Rad51-ssDNA presynaptic filament causes the generation of form U (Fig. 3Bc, lanes 4-6), indicating the transfer of Rad51 from the presynaptic filament to the dsDNA. The addition of RPA further stimulates the Srs2-mediated release of Rad51 from the presynaptic filament and the formation of form U (Fig. 3Bc, lanes 8-10). RPA has high affinity for ssDNA and it can compete with Rad51 for binding to ssDNA^{10,19,20}. The enhanced production of form U was therefore probably due to the sequestering of ssDNA by RPA after Srs2 had released Rad51, thereby preventing the renucleation of Rad51 on the ssDNA. This premise was verified by electron microscopy and explains the

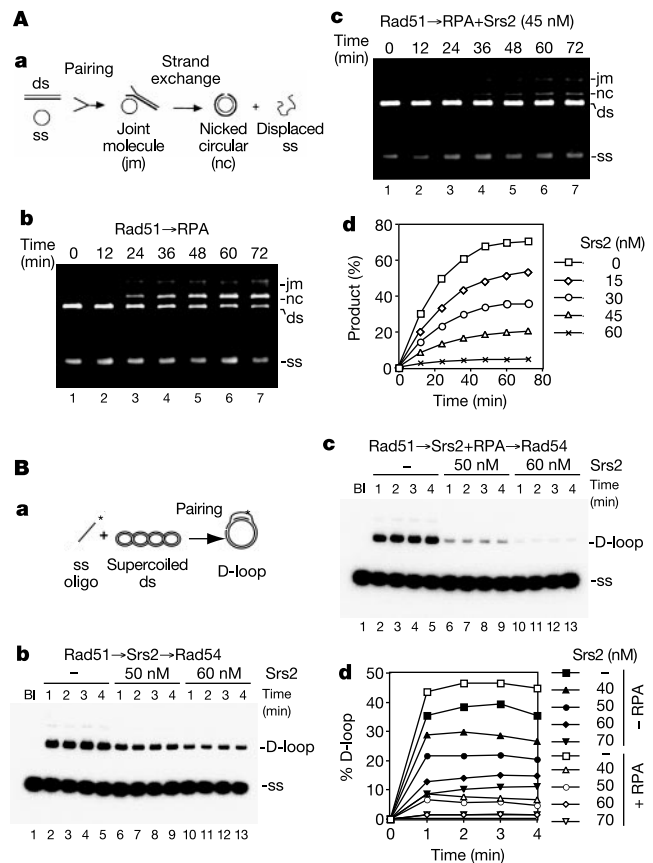


Figure 2 Srs2 inhibits Rad51-mediated DNA pairing and strand exchange. **A**, **a**, The DNA strand exchange scheme. In **b**, the DNA substrates were incubated with Rad51 and RPA. In **c**, Srs2 was also included. The results from **b** and **c** and from reactions with other Srs2 amounts are plotted in **d**. **B**, **a**, The D-loop reaction scheme. In **b**, Rad51, Srs2 and Rad54 were incubated with the DNA substrates. In **c**, RPA was also included. The results from **b** and **c** and from reactions with other Srs2 amounts are plotted in **d**. Filled symbols, reactions without RPA; open symbols, reactions with RPA.

RPA-mediated enhancement of the inhibitory effect of Srs2 in the D-loop reaction (Fig. 2B).

The Srs2-mediated disruption of the Rad51 presynaptic filament was examined by a second approach. Here, Rad51 that had been dissociated from ssDNA by Srs2 was trapped on a DNA duplex bound to magnetic beads through a biotin–streptavidin linkage (Fig. 3Ca). Rad51 was eluted from the bead-bound DNA duplex by treatment with SDS and then analysed in a denaturing polyacrylamide gel. Consistent with results from the topoisomerase I-linked assay (Fig. 3B) was the observation that there was an Srs2-concentration-dependent transfer of Rad51 from the presynaptic filament to the bead-bound DNA duplex (Fig. 3Cb).

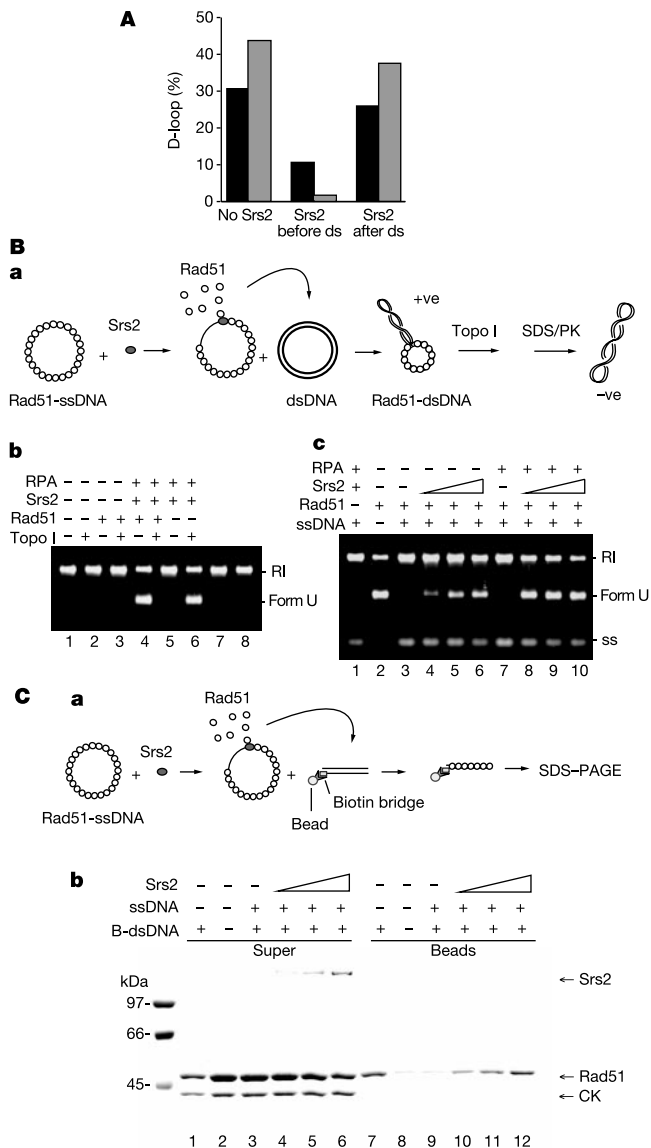


Figure 3 Srs2 disrupts the Rad51 presynaptic filament. **A**, D-loop reactions without and with Srs2 added before or after the duplex substrate were performed. The reactions were repeated with RPA present. Black bars, reactions without RPA; grey bars, reactions with RPA. **B**, **a**, The reaction scheme. PK, proteinase K. **b**, Only Rad51 makes form U. In **c**, Rad51 presynaptic filaments, assembled with or without RPA, were treated with Srs2 and topoisomerase. Lane 2 contained form U marker. RI, relaxed duplex; ss, single-stranded DNA. **C**, **a**, The reaction scheme. In **b**, Rad51 presynaptic filaments were incubated with Srs2 and then with beads containing dsDNA. Rad51 was also incubated with beads containing dsDNA (lanes 1 and 7) and beads without DNA (lanes 2 and 8). The supernatant and bead fractions were analysed. CK, creatine kinase.

Last, we used electron microscopy to characterize the action of Srs2 on the Rad51 presynaptic filament. After incubation of Rad51 with circular ssDNA, abundant presynaptic filaments^{17,18} were seen (Fig. 4a). Under the same conditions, RPA formed complexes with ssDNA that appeared as compact structures with distinctive protein bulges (Fig. 4b). Although RPA alone was unable to disrupt the Rad51 presynaptic filaments (Fig. 4c), the addition of Srs2 with RPA to the presynaptic filaments caused a complete loss of the filaments, and the concomitant formation of RPA–ssDNA complexes (Fig. 4d). Previous biochemical experiments had shown transfer of Rad51 from the presynaptic filament to dsDNA promoted by Srs2 (Fig. 3B and C). This Srs2-mediated transfer of Rad51 to dsDNA could be observed directly by electron microscopy (Fig. 4e). The data from the electron microscopic analyses agree with results from the biochemical experiments (Figs 2 and 3), because they show that Srs2 disrupts the Rad51 presynaptic filament.

Even though homologous recombination is important for repairing DNA strand breaks induced by ionizing radiation and endogenous agents, and for restarting delinquent DNA replication forks, it can also generate deleterious genomic rearrangements and create DNA structures that cannot be properly resolved¹. Cells have therefore evolved mechanisms to avoid untimely recombination^{1,5}. Our studies provide evidence that Srs2 does this by disrupting the Rad51 presynaptic filament. The same conclusion has been reached independently²¹. Furthermore, even though RPA can function as a cofactor in the assembly of the Rad51 presynaptic filament^{10,20}, it might also promote the anti-recombination function of Srs2 by preventing reassembly of the presynaptic filament (Figs 3 and 4). That Srs2 uses the free energy from ATP hydrolysis to dislodge Rad51 from the presynaptic filament has been verified with mutant variants of Srs2 (srs2 K41A and srs2 K41R) defective for ATP hydrolysis. The physical interaction noted between Rad51 and Srs2 further suggests a mechanism for targeting the latter to the presynaptic filament. Taken together, the results presented here indicate that the motor activity of Srs2 driven by ATP hydrolysis is capable of dissociating not only DNA structures⁶ but also DNA–protein complexes.

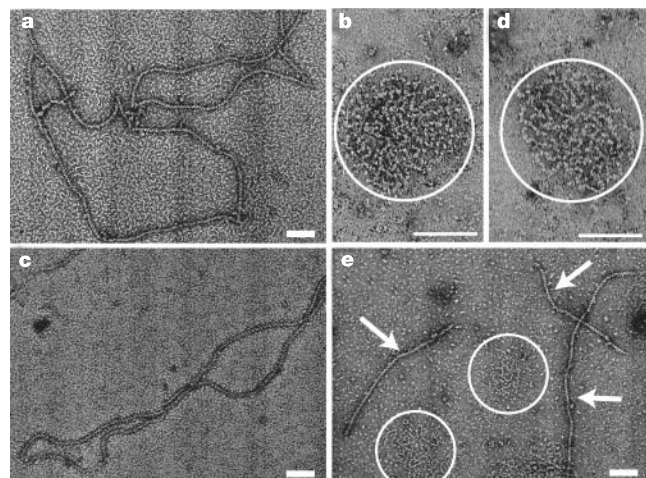


Figure 4 EM analysis of Rad51 filament disruption by Srs2. **a**, **b**, Rad51 (**a**) and RPA (**b**) were each incubated with ssDNA; examples of the nucleoprotein complexes that formed are shown. **c**, RPA was not able to disrupt preformed Rad51 filaments; an example of the Rad51 filaments present is shown. **d**, Incubation of preformed Rad51 filaments with Srs2 and RPA caused the loss of filaments and concomitant formation of RPA–ssDNA complexes, an example of which is shown. **e**, When preformed Rad51–ssDNA filaments were incubated with Srs2, RPA and linear duplex, RPA–ssDNA complexes were formed (circled) and transfer of Rad51 onto the linear duplex was visualized (arrows). Scale bars, 100 nm.

The inhibitory effect of Srs2 on Rad51-mediated DNA strand exchange can be partly overcome by the inclusion of Rad52 protein, a recombination mediator that promotes Rad51 presynaptic filament assembly^{11,12}. However, the Rad55–Rad57 complex, which also has recombination mediator activity^{11,12}, is much less effective in alleviating the inhibitory effect of Srs2. Furthermore, Rad52 and the Rad55–Rad57 complex do not seem to act synergistically. Interestingly, we have found that Srs2 can also dismantle presynaptic filaments of RecA and human Rad51 proteins. It therefore seems that the presynaptic filaments formed by the RecA/Rad51 class of general recombinases share a conserved feature that is recognized by Srs2, making them prone to disruption by the motor activity of Srs2.

The sensitivity of *srs2* mutants to DNA-damaging agents^{6,22} is alleviated by deleting *RAD51* (ref. 23), and the inability to remove Rad51 from DNA in the *srs2* mutants most probably accounts for the hyper-recombination phenotype of these mutants¹. Similarly, the cell cycle checkpoint recovery and adaptation defect in *srs2* mutants might be related to an inability to evict Rad51 from damaged DNA². Cells mutated for *SRS2* grow slowly, exhibit an extended late S and/or G2 phase, and are defective in meiosis²⁵. These defects could result from the generation of unresolvable recombination intermediates that trigger checkpoint activation and thereby compromise cell cycle progression. In addition to functioning as an anti-recombinase, Srs2 could conceivably prevent D-loop reversal by removing Rad51 bound to the displaced ssDNA strand. The various activities of Srs2 might be subject to modulation by phosphorylation²⁴.

Other DNA helicase enzymes are known to suppress recombination in eukaryotic cells, including the *S. cerevisiae* Sgs1 protein and the human BLM and WRN proteins, mutated in Bloom's syndrome and Werner's syndrome, respectively. Untimely and aberrant recombination events in Bloom's syndrome and Werner's syndrome cells could contribute to the genomic instability in these cells²⁶. It has been suggested that BLM and WRN proteins control the level of recombination by dissociating recombination intermediates^{5,27}. It will be of interest to test whether Sgs1, BLM and WRN proteins affect the integrity of the hRad51 presynaptic filament, as over-expression of Sgs1 protein can partly suppress some of the defects of *srs2* mutants²⁸. □

Methods

Antibodies and Srs2 purification

Polyclonal antiserum was raised against residues 177–646 of Srs2 fused to glutathione S transferase. Antibodies were purified from the rabbit anti-serum by affinity chromatography on a column containing the antigen crosslinked to cyanogen bromide-activated sepharose 4B matrix (Amersham Biosciences). *SRS2* gene was placed under the T7 promoter in the vector pET11c to yield plasmid pET11c::Srs2, which was introduced into *E. coli* BL21 (DE3). Srs2 expression was induced by isopropyl β-D-thiogalactoside, and extract from 70 l of culture was subjected to precipitation with ammonium sulphate and chromatographic fractionation in columns of Q Sepharose, SP Sepharose, hydroxyapatite and Mono Q. The final Srs2 pool (300 μg at 2 mg ml⁻¹) was nearly homogeneous and stored in small portions at -80 °C.

DNA substrates

The φX circular (+) strand was from New England Biolabs. The φX replicative form I DNA (Gibco-BRL) was linearized by digestion with *Apa*LI. The pBluescript SK(-) replicative form I DNA was prepared as described²⁹. Oligonucleotide D1 has the sequence: 5'-AAATCAATCTAAAGTATATATGAGTAAACTTGGTCTGACAGTTACCAATGCTTAA TCAGTGAGGCACCTATCTCAGCGATCTGTCTATT-3', being complementary to positions 1932–2022 of the pBluescript replicative form I DNA. Oligonucleotide H2 has the sequence: 5'-GTAAGTGCAGACCAAGTTTACTCATATATACTTTGATTGATT-3', being complementary to the first 45 residues of oligonucleotide D1. The two oligonucleotides were 5' end-labelled with [γ-³²P]ATP and purified as described²⁹. The DNA helicase substrate was obtained by hybridizing D1 to radiolabelled H2, as described¹⁴.

Biotinylated dsDNA coupled to magnetic beads

The ends of a 769-base pair fragment derived from digesting φX174 replicative form I DNA with *Apa*LI and *Xho*I were filled in with the Klenow polymerase, using a mixture of dGTP, dTTP, Bio-7-dATP and Bio-11-dCTP (Enzo Diagnostics). The biotinylated DNA

fragment was immobilized on streptavidin-coated magnetic beads (Roche Molecular Biochemicals) to give biotinylated DNA at 40 ng μl⁻¹ packed volume.

Binding of Srs2 to beads containing Rad51

Rad51 and BSA were coupled to Affi-Gel 15 beads (Bio-Rad) at 5 and 12 mg ml⁻¹, respectively¹⁴. To examine Srs2 binding, 3 μg Srs2 was mixed with 7 μl Affi-Rad 51 or Affi-BSA beads in 30 μl PBS (10 mM KH₂PO₄ pH 7.2, 150 mM KCl, 1 mM dithiothreitol (DTT) and 0.01% Igepal) at 4 °C for 30 min. The beads were collected by centrifugation; after the supernatant had been decanted off, the beads were washed twice with 100 μl buffer, then treated for 5 min with 30 μl 2% SDS at 37 °C to elute bound Srs2. The various fractions—10 μl each—were analysed by immunoblotting to determine their Srs2 content.

Yeast two-hybrid assay

RAD51 was cloned into pGAD10, which contains the *GAL4* transcription activation domain, and the resulting plasmid was introduced into the haploid yeast strain PJ69-4a (ref. 30). *SRS2* (residues 1–1174), two C-terminal fragments of *SRS2* (residues 783–1174 and residues 738–998), and *RAD52* were cloned into pGBKT7, which contains the *GAL4* DNA-binding domain; the resulting plasmids were introduced into the haploid yeast strain PJ69-4α (ref. 30). Diploid strains obtained by mating plasmid-bearing PJ69-4a and PJ69-4α haploids were grown on synthetic medium lacking tryptophan and leucine. To select for two-hybrid interactions, which would result in the activation of the *ADE2* and *HIS3* reporter genes, diploid cells were replica-plated on synthetic medium lacking tryptophan, leucine and adenine, and also on synthetic medium lacking tryptophan, leucine and histidine³⁰. Both platings gave identical results. Only the plating on the tryptophan, leucine and adenine dropout medium is shown in Fig. 1e.

DNA helicase assay

Srs2 (35 nM) was incubated at 30 °C for 10 min with the DNA substrate (300 nM nucleotides) in 10 μl buffer H (25 mM Tris-HCl pH 7.5, 2.5 mM MgCl₂, 1 mM DTT, 100 μg ml⁻¹ BSA) containing 2 mM ATP or β-γ-imidoadenosine 5'-phosphate (AMP-PNP) and then analysed¹⁴.

Homologous DNA pairing and strand exchange reaction

Buffer R (35 mM Tris-HCl pH 7.4, 2.0 mM ATP, 2.5 mM MgCl₂, 50 mM KCl, 1 mM DTT, containing an ATP-regenerating system consisting of 20 mM creatine phosphate and 20 μg ml⁻¹ creatine kinase) was used for the reactions, and all the incubation steps were performed at 37 °C. Rad51 (10 μM) was mixed with φX circular (+) strand (30 μM nucleotides) in 30 μl for 5 min, followed by the incorporation of RPA (2 μM) in 1.5 μl and a 3 min incubation. The reaction was completed by adding 3 μl 50 mM spermidine hydrochloride and linear φX dsDNA (30 μM nucleotides) in 3 μl. Portions (4.5 μl) of the reaction mixtures were taken at the indicated times, deproteinized and resolved in agarose gels followed by ethidium bromide staining of the DNA species, as described previously¹⁸. Srs2 was added to the reactions in 0.9 μl at the time of RPA incorporation.

D-loop reaction

Buffer R was used for the D-loop reactions. The radiolabelled oligonucleotide D1 (3 μM nucleotides) was incubated with Rad51 (1 μM) in 22 μl for 5 min at 37 °C, followed by the incorporation of Rad54 (150 nM) in 1 μl and a 2-min incubation at 23 °C. The reaction was initiated by adding pBluescript replicative form I DNA (50 μM base pairs) in 2 μl. The reaction mixtures were incubated at 30 °C, and 5-μl aliquots were withdrawn at the indicated times and processed for electrophoresis as described above. The gels were dried and subjected to phosphorimaging analysis. The percentage of D-loop refers to the quantity of the replicative form substrate that had been converted into D-loop. When present, RPA (200 nM) and Srs2 (40–70 nM) were added to the preassembled Rad51 filament, followed by a 4-min incubation at 37 °C before Rad54 was incorporated. In Fig. 3A, Srs2 (45 nM) was added to the D-loop reactions before Rad54 as above, or 1 min after the incorporation of the duplex substrate. The reactions were terminated after 4 min of incubation.

Topoisomerase-I-linked DNA unwinding assay

Buffer R was used for the reactions and all the incubation steps were performed at 37 °C. Rad51 (4 μM) was incubated for 4 min with pBluescript (-) strand (20 μM nucleotides) in 7.8 μl. Srs2 (40, 60 or 80 nM) and RPA (1 μM) were added in 1 μl, followed by a 4-min incubation. Topologically relaxed φX174 DNA (12.5 μM nucleotides) in 0.8 μl and 2.5 U calf thymus topoisomerase I (Invitrogen) in 0.4 μl storage buffer were then incorporated to complete the reaction. The reaction mixtures were incubated for 8 min and then stopped by adding SDS to 0.5%. In reactions that did not contain the (-) strand, Rad51, with or without RPA (1 μM) and Srs2 (80 nM), was incubated for 8 min with topologically relaxed φX174 DNA and topoisomerase I in a final volume of 10 μl. The reaction mixtures were treated for 10 min with proteinase K (0.5 mg ml⁻¹) before being analysed in 0.9% agarose gels.

Transfer of Rad51 to bead-bound biotinylated dsDNA

M13mp18 circular (+) strand (7.2 μM nucleotides) was incubated for 5 min with Rad51 (2.4 μM) at 37 °C, followed by the addition of Srs2 (30, 60 or 90 nM) in a final volume of 20 μl buffer R containing 50 mM KCl and 0.01% Igepal. After 3 min at 37 °C, 4 μl magnetic beads containing dsDNA were added to the reaction, followed by constant mixing for 5 min at 23 °C. The beads were captured with the Magnetic Particle Separator (Boehringer Mannheim), washed twice with 50 μl buffer, and the bound Rad51 was eluted with 20 μl 1% SDS. The supernatant, which contained unbound Rad51, and the SDS eluate (10 μl each) were analysed by SDS-polyacrylamide-gel electrophoresis (SDS-PAGE).

Electron microscopy

The reactions were performed in buffer R at 37 °C and had a final volume of 12.5 µl. To assemble the Rad51 presynaptic filament, M13mp18 (+) strand (7.2 µM nucleotides) and 1.3 µg Rad51 (2.4 µM) were incubated for 5 min. To test the effects of Srs2 and RPA, these proteins were added to the reaction mixtures containing the preassembled Rad51 presynaptic filament to final concentrations of 60 nM (Srs2) and 350 nM (RPA), followed by a 3-min incubation. In some cases, linear dsDNA (a 5.2-kilobase fragment derived from the pET24 vector) was also added with Srs2 and RPA to 7.2 µM base pairs, followed by a 5-min incubation. For electron microscopy, 3 µl of each reaction mixture was applied to copper grids coated with thin carbon film after glow-discharging the coated grids for 2 min. The grids were washed twice with buffer R and stained for 30 s with 0.75% uranyl formate. After air-drying, the grids were examined with a Philips Tecnai12 electron microscope under low-dose conditions. Images were recorded either with a charge-coupled device camera (Gatan) or on Kodak SO-163 films at × 30,000 magnification and then scanned on a SCAI scanner (Zeiss). The experiments shown in Fig. 4 were each independently repeated three or more times and at least 100 nucleoprotein complexes were examined in each experiment.

Received 3 February; accepted 20 March 2003; doi:10.1038/nature01577.

1. Klein, H. L. A radical solution to death. *Nature Genet.* **25**, 132–134 (2000).
2. Vaze, M. B. *et al.* Recovery from checkpoint-mediated arrest after repair of a double-strand break requires Srs2 helicase. *Mol. Cell* **10**, 373–385 (2002).
3. Lee, S. K., Johnson, R. E., Yu, S. L., Prakash, L. & Prakash, S. Requirement of yeast SGS1 and SRS2 genes for replication and transcription. *Science* **286**, 2339–2342 (1999).
4. Gangloff, S., Soustelle, C. & Fabre, F. Homologous recombination is responsible for cell death in the absence of the Sgs1 and Srs2 helicases. *Nature Genet.* **25**, 192–194 (2000).
5. Oakley, T. J. & Hickson, I. D. Defending genome integrity during S-phase: putative roles for RecQ helicases and topoisomerase III. *DNA Repair* **1**, 175–207 (2002).
6. Rong, L. & Klein, H. L. Purification and characterization of the SRS2 DNA helicase of the yeast *Saccharomyces cerevisiae*. *J. Biol. Chem.* **268**, 1252–1259 (1993).
7. Milne, G. T., Ho, T. & Weaver, D. T. Modulation of *Saccharomyces cerevisiae* DNA double-strand break repair by SRS2 and RAD51. *Genetics* **139**, 1189–1199 (1995).
8. Chanet, R., Heude, M., Adjiri, A., Maloisel, L. & Fabre, F. Semidominant mutations in the yeast Rad51 protein and their relationships with the Srs2 helicase. *Mol. Cell. Biol.* **16**, 4782–4789 (1996).
9. Schild, D. Suppression of a new allele of the yeast RAD52 gene by overexpression of RAD51, mutations in srs2 and ccr4, or mating-type heterozygosity. *Genetics* **140**, 115–127 (1995).
10. Sung, P. Catalysis of ATP-dependent homologous DNA pairing and strand exchange by yeast RAD51 protein. *Science* **265**, 1241–1243 (1994).
11. Sung, P., Trujillo, K. M. & Van Komen, S. Recombination factors of *Saccharomyces cerevisiae*. *Mutat. Res.* **451**, 257–275 (2000).
12. Cox, M. M. Recombinational DNA repair of damaged replication forks in *Escherichia coli*: questions. *Annu. Rev. Genet.* **35**, 53–82 (2001).
13. Bianco, P. R., Tracy, R. B. & Kowalczykowski, S. C. DNA strand exchange proteins: a biochemical and physical comparison. *Front. Biosci.* **3**, 570–603 (1998).
14. Petukhova, G., Stratton, S. & Sung, P. Catalysis of homologous DNA pairing by yeast Rad51 and Rad54 proteins. *Nature* **393**, 91–94 (1998).
15. Mazin, A. V., Zaitseva, E., Sung, P. & Kowalczykowski, S. C. Tailed duplex DNA is the preferred substrate for Rad51 protein-mediated homologous pairing. *EMBO J.* **19**, 1148–1156 (2000).
16. Van Komen, S., Petukhova, G., Sigurdsson, S. & Sung, P. Functional cross-talk among Rad51, Rad54, and replication protein A in heteroduplex DNA joint formation. *J. Biol. Chem.* **277**, 43578–43587 (2002).
17. Ogawa, T., Yu, X., Shinohara, A. & Egelman, E. H. Similarity of the yeast RAD51 filament to the bacterial RecA filament. *Science* **259**, 1896–1899 (1993).
18. Sung, P. & Roberson, D. L. DNA strand exchange mediated by a RAD51-ssDNA nucleoprotein filament with polarity opposite to that of RecA. *Cell* **82**, 453–461 (1995).
19. Sung, P. Yeast Rad55 and Rad57 proteins form a heterodimer that functions with replication protein A to promote DNA strand exchange by Rad51 recombinase. *Genes Dev.* **11**, 1111–1121 (1997).
20. Sugiyama, T., Zaitseva, E. M. & Kowalczykowski, S. C. A single-stranded DNA-binding protein is needed for efficient presynaptic complex formation by the *Saccharomyces cerevisiae* Rad51 protein. *J. Biol. Chem.* **272**, 7940–7945 (1997).
21. Veaute, X. *et al.* The Srs2 helicase prevents recombination by disrupting Rad51 nucleoprotein filaments. *Nature* **423**, 309–312 (2003).
22. Aboussekhra, A. *et al.* RADH, a gene of *Saccharomyces cerevisiae* encoding a putative DNA helicase involved in DNA repair. Characteristics of radH mutants and sequence of the gene. *Nucleic Acids Res.* **17**, 7211–7219 (1989).
23. Aboussekhra, A., Chanet, R., Adjiri, A. & Fabre, F. Semidominant suppressors of Srs2 helicase mutations of *Saccharomyces cerevisiae* map in the RAD51 gene, whose sequence predicts a protein with similarities to prokaryotic RecA proteins. *Mol. Cell. Biol.* **12**, 3224–3234 (1992).
24. Liberi, G. *et al.* Srs2 DNA helicase is involved in checkpoint response and its regulation requires a functional Mec1-dependent pathway and Cdk1 activity. *EMBO J.* **19**, 5027–5038 (2000).
25. Palladino, F. & Klein, H. L. Analysis of mitotic and meiotic defects in *Saccharomyces cerevisiae* SRS2 DNA helicase mutants. *Genetics* **132**, 23–37 (1992).
26. Adams, M. D., McVey, M. & Sekelsky, J. J. *Drosophila* BLM in double-strand break repair by synthesis-dependent strand annealing. *Science* **299**, 265–267 (2003).
27. Wu, L., Davies, S. L., Levitt, N. C. & Hickson, I. D. Potential role for the BLM helicase in recombinational repair via a conserved interaction with RAD51. *J. Biol. Chem.* **276**, 19375–19381 (2001).
28. Mankouri, H. W., Craig, T. J. & Morgan, A. SGS1 is a multicopy suppressor of srs2: functional overlap between DNA helicases. *Nucleic Acids Res.* **30**, 1103–1113 (2002).
29. Petukhova, G., Stratton, S. A. & Sung, P. Single strand DNA binding and annealing activities in the yeast recombination factor Rad59. *J. Biol. Chem.* **274**, 33839–33842 (1999).
30. Krejci, L., Damborsky, J., Thomsen, B., Duno, M. & Bendixen, C. Molecular dissection of interactions between Rad51 and members of the recombination-repair group. *Mol. Cell. Biol.* **21**, 966–976 (2001).

Acknowledgements We thank M. Sehorn and K. Trujillo for reading the manuscript. This work was supported by research grants from the NIH (H.K., T.E. and P.S.). S.V.K. was supported in part by a predoctoral fellowship from the US Department of Defense, and Y.L. was supported by a NIH postdoctoral fellowship. The molecular electron microscopy facility at Harvard Medical School was established by a donation from the Giovanni Armeise Harvard Center for Structural Biology, and is maintained through a NIH grant.

Competing interests statement The authors declare that they have no competing financial interests.

Correspondence and requests for materials should be addressed to L.K. (krejci@uthscsa.edu) or P.S. (sung@uthscsa.edu).

The Srs2 helicase prevents recombination by disrupting Rad51 nucleoprotein filaments

Xavier Veaute*, Josette Jousset†, Christine Soustelle*‡, Stephen C. Kowalczykowski§, Eric Le Cam† & Francis Fabre*

* CEA, DSV, Département de Radiobiologie et Radiopathologie, UMR217 CNRS/CEA, BP6, 92265 Fontenay aux Roses Cedex, France

† Interactions Moléculaires et Cancer, UMR 81126 CNRS/IGR/UPS, Institut Gustave Roussy, Rue Camille Desmoulins, 94805 Villejuif Cedex, France
 § Sections of Microbiology and of Molecular and Cellular Biology, Center for Genetics and Development, University of California, Davis, California 95616-8665, USA

Homologous recombination is a ubiquitous process with key functions in meiotic and vegetative cells for the repair of DNA breaks. It is initiated by the formation of single-stranded DNA on which recombination proteins bind to form a nucleoprotein filament that is active in searching for homology, in the formation of joint molecules and in the exchange of DNA strands¹. This process contributes to genome stability but it is also potentially dangerous to cells if intermediates are formed that cannot be processed normally and thus are toxic or generate genomic rearrangements. Cells must therefore have developed strategies to survey recombination and to prevent the occurrence of such deleterious events. In *Saccharomyces cerevisiae*, genetic data have shown that the Srs2 helicase negatively modulates recombination^{2,3}, and later experiments suggested that it reverses intermediate recombination structures^{4–7}. Here we show that DNA strand exchange mediated *in vitro* by Rad51 is inhibited by Srs2, and that Srs2 disrupts Rad51 filaments formed on single-stranded DNA. These data provide an explanation for the anti-recombinogenic role of Srs2 *in vivo* and highlight a previously unknown mechanism for recombination control.

Several phenotypes (discussed below) conferred by the *srs2* deletion are suppressed by mutations that prevent formation of the Rad51 nucleofilaments^{8,9}. Two hypotheses could explain this suppression: either Srs2 functions in replication and repair to prevent the formation of toxic recombination structures, or Srs2 disrupts dead-end recombination intermediates, possibly formed after the arrest of the replication fork, to allow repair through alternative pathways. This second proposition led us to ask whether purified Srs2 acts on preformed recombination structures.

Srs2 was expressed from a baculovirus vector in which SRS2 was cloned in frame with a histidine tag at its amino terminus. We showed that the protein fusion expressed in yeast fully complements the sensitivity of *srs2*-deleted cells to radiation (data not shown).

‡ Present address: UMR2167 CNRS Centre de Génétique Moléculaire, Bâtiment 26, avenue de la Terrasse, 91198 Gif-sur-Yvette Cedex, France.